Endo180 (*MRC2*) antibody-drug conjugate for the treatment of sarcoma

Rachel J. Evans[1], Douglas W. Perkins[1], Joanna Selfe[2], Anna Kelsey[3], Gavin P. Birch[4], Janet M. Shipley[2], Koen Schipper[1] and Clare M. Isacke[1]

[1]The Breast Cancer Now Toby Robins Research Centre, The Institute of Cancer Research, London SW3 6JB, UK

[2]Sarcoma Molecular Pathology Team, Divisions of Molecular Pathology and Cancer Therapeutics, The Institute of Cancer Research, London, UK

[3]Department of Paediatric Pathology, University of Manchester Foundation Trust, Manchester, UK.

[4]Abzena (Cambridge) Ltd. Babraham Research Campus, Babraham, Cambridge, CB22 3AT, UK

Running title: Endo180 ADC for the treatment of sarcoma

Abbreviations:

ADC – Antibody-drug conjugate

CAF – Cancer-associated fibroblast

CTLD – C-type lectin-like domain

DAR – Drug to antibody ratio

mAb – Monoclonal antibody

MMAE – Monomethyl auristatin E

STS – Soft tissue sarcoma

TMA – Tissue microarray

***Corresponding Author**: Clare M. Isacke, The Breast Cancer Now Toby Robins Research Centre, The Institute of Cancer Research, 237 Fulham Road, London SW3 6JB, UK. Telephone +44 20 7153 5510, Email clare.isacke@icr.ac.uk

Conflicts of interest Statement: Gavin P. Birch is a full-time employee of Abzena (Cambridge) Ltd. The other authors have no conflicts of interest to declare.

Abstract

Although the 5-year survival rates for sarcoma patients have improved, the proportion of patients relapsing after first line treatment remains high and survival of patients with metastatic disease is dismal. Moreover, the extensive molecular heterogeneity of the multiple different sarcoma subtypes poses a substantial challenge to developing more personalized treatment strategies. From immunohistochemical staining of a large set of 625 human soft tissue sarcomas we demonstrate strong tumor cell staining of the Endo180 (*MRC2*) receptor in a high proportion of samples, findings echoed in gene expression datasets showing a significantly increased expression in both soft tissue and bone sarcomas compared to normal tissue. Endo180 is a constitutively recycling transmembrane receptor and therefore an ideal target for an antibody-drug conjugate (ADC). An anti-Endo180 monoclonal antibody conjugated to the anti-mitotic agent, MMAE via a cleavable linker, is rapidly internalized into target cells and trafficked to the lysosome for degradation, causing cell death specifically in Endo180 expressing sarcoma cell lines. In a sarcoma tumor xenograft model, the Endo180-vc-MMAE ADC, but not an Isotype-vc-MMAE control or the unconjugated Endo180 antibody, drives on-target cytotoxicity resulting in tumor regression and a significant impairment of metastatic colonization of the lungs, liver and lymph nodes. These data, together with the lack of a phenotype in mice with an *Mrc2* genetic deletion, provide pre-clinical proof-of-principle evidence for the future development of an Endo180-ADC as a therapeutic strategy in a broad range of sarcoma subtypes and, importantly, with potential impact both on the primary tumor and in metastatic disease.

Introduction

Sarcomas represent over 100 different cancer subtypes which derive from mesenchymal cells in bone, cartilage or connective tissues and are broadly categorized as either soft tissue sarcomas (STS) or bone sarcomas (1,2). Although sarcomas are relatively rare, causing less than 1% of adult cancers, some subtypes, such as rhabdomyosarcomas, predominantly affect under 20 year olds. Together, sarcomas are responsible for 12% of childhood and young adult cancers (3). The current standard of care for adults with localized disease is surgery with or without radiation, however patients with unresectable or metastatic disease also receive chemotherapy and radiotherapy (4). Despite intensive treatment, greater than 50% of patients with high grade STS develop metastatic disease resulting in a median overall survival of 19-20 months (5). The 5 year overall survival for patients with metastatic bone sarcoma is 30% (6,7). In recent years, there has been renewed activity in using immunotherapies to target sarcoma. In total, 9 immunoconjugates targeting sarcomas have entered clinical trials, 7 antibody-drug conjugates (ADCs) and 2 radioimmunoconjugates, although none have yet been approved for clinical use (8). Therefore, despite these advances there remains a significant unmet clinical need to identify effective therapeutic targets in sarcoma, especially in the metastatic setting.

Endo180 (gene name *MRC2*, also known as uPARAP, CD280 and TEM1) is a member of the mannose receptor family containing an N-terminal cysteine-rich domain, a collagen-binding fibronectin type II domain (9,10), 8 C-type lectin-like domains (CTLDs), a single transmembrane domain and a short cytoplasmic domain which mediates receptor internalization (11) (Fig. 1a). In adults, expression of Endo180 is largely restricted to normal tissue fibroblasts but expression is upregulated on cancer-associated fibroblasts (CAFs) and particularly the subset of myofibroblastic CAFs (12,13). Importantly, mice with a whole-body genetic deletion of Endo180 have no overt phenotype (14,15) however when implanted with syngeneic tumor cells show

impaired tumor progression and a reduction in viable CAFs (13). In addition to CAFs, Endo180 receptor expression has also been reported on tumor cells of mesenchymal origin including glioblastoma, metaplastic breast cancer, mesothelioma and sarcomas, both bone and soft tissue (16-21).

ADCs are a tripartite structure consisting of an antibody, a linker and a payload. Often these payloads are drugs up to 1000-fold more toxic than agents used in chemotherapy (22). Therefore, these drugs cannot be used systemically and require coupling to antibodies to direct the cytotoxic effect to specific targets and prevent exposure of healthy tissue. Whilst the clinical efficacy of ADCs is well demonstrated against hematological and epithelial cancers they have had little success in the context of mesenchymal tumors. Of the monoclonal antibodies (mAbs) raised against Endo180 in the original screen (23), one of these, mAb A5/158, was used here to generate an ADC. A5/158 has been extensively characterized (10,24), and is specific for human Endo180 with its epitope located within CTLD2 (Fig. 1a). Endo180 is rapidly and constitutively recruited into clathrin coated pits resulting in >50% of the receptor being internalized into intracellular endosomes within 2 minutes (11,23). Inside the endosomes, the low pH environment results in ligand dissociation and recycling of Endo180 back to the plasma membrane, making it ideal for rapid uptake of an ADC.

Here, we show high levels of Endo180 protein in the majority of STS of different subtypes, and upregulated *MRC2* expression in multiple sarcoma datasets. Experimentally, an Endo180 ADC demonstrates target-dependent cytotoxicity of multiple sarcoma cell lines *in vitro* and tumor regression and impairment of metastasis in an *in vivo* sarcoma model.

Materials and Methods

Reagents and cells

Antibodies and the dilutions used are described in Supplementary Table S1. MG-63, HT-1080, MCF-7 and HT-29 cells were from Isacke laboratory stocks. A-204, G-402, SK-UT-1 and SJSA-1 cells were from Paul Huang (ICR) laboratory stocks. MG-63 cells were transduced with a luciferase2-mCherry vector (mChLuc2). mCherry+ MG-63 cells were enriched by fluorescence-activated cell sorting (FACS). All cells were short tandem repeat tested (StemElite ID System; Promega) and tested negative in routine bi-monthly tests for mycoplasma contamination (MycoAlert; Lonza) (last date tested 22nd July 2022). All cell lines were used between 2-15 passages after thawing. The generation of anti-human Endo180 mouse mAbs A5/158 and 39.10 have been described previously (23,24). Antibody concentration was determined by Coomassie Blue or Instant Blue staining of reduced SDS-PAGE gels and interpolation from a standard curve of light chains of either isotype control antibody (BioLegend, 401408) or trastuzumab (Roche, N3031H02).

Tissue microarrays (TMAs). All TMAs were constructed as described (25). Details of the rhabdomyosarcoma and adult soft tissue sarcoma TMAs and associated ethical approvals have been reported previously (26,27). TMAs had one to five assessable cores per patient sample. The liposarcoma TMAs were constructed with 1 mm diameter cores and comprised cores from tumor biopsies of patients with well-differentiated or dedifferentiated liposarcoma and normal fat samples. Multiple cores were taken from each sample. Where tumor samples contained both well-differentiated and dedifferentiated components, cores from both components were represented on the arrays. Tumor diagnoses had been previously confirmed by a specialist soft tissue pathologist.

Staining of the TMA sections (4 μm) with the anti-human Endo180 mAb 39.10 was as described previously (24). In brief, slides were incubated with Dako REAL Peroxidase Block (Agilent, S2023) for 5 min followed by 39.10 for 1 h at room temperature. Detection was achieved using Dako Mouse EnVision reagent (Agilent, K4001) for 30 min, counterstained using Dako FLEX hematoxylin (Agilent, K8008) and visualized using Dako DAB+ (Agilent, K3468). Positive and negative control samples were included in each run. Stained TMAs were reviewed by a Consultant Pediatric Histopathologist (AK). The staining was both cytoplasmic and perinuclear, and some cases had dot like accentuation. Cellularity varied depending on sarcoma subtype. Cases with strong 3+ or moderate 2+ immunostaining were scored as positive (majority of tumor cells in all replicate cores staining Endo180-positive) or negative (no or low level (1+) Endo180 staining on tumor cells). TMA cores with only stromal Endo180 expression were scored negative. TMA cores with equivocal staining or replicate cores with non-concurrent Endo180 staining were not scored.

In vitro studies

Immunofluorescence staining. For immunofluorescence staining of fixed cells, 2 x 10^5 cells were cultured for 2 days on glass coverslips in a 6 cm dish before fixing in 4% paraformaldehyde. Cells were permeabilized in 0.5% Triton X 100 and stained with A5/158 or isotype control antibodies, Alexa dye-labeled phalloidin (ThermoFisher, A22283) and DAPI (Invitrogen, D1306). For immunofluorescence staining of live cells, 2 x 10^5 cells were cultured for 2 days on glass coverslips in a 6 cm dish. A5/158 and isotype control antibodies were conjugated to Alexa Fluor 488 dye (ThermoFisher, A20181) as per the manufacturer's protocol. Directly conjugated antibodies were diluted in binding buffer (DMEM, 10 mM HEPES pH 7.5, 2 mg/mL BSA (Sigma, A2153)) and incubated with cells for 1 h at 4°C. Coverslips were washed and incubated with LysoTracker Red DND-99 (ThermoFisher) and Hoechst 3342 nuclear stain (ThermoFisher) in binding buffer for 30 min at 37°C. Cells were washed in binding

buffer and fixed in 4% paraformaldehyde. All fluorescence images were collected on a Leica TCS SP8 confocal microscope.

Western blotting. Cells were grown to 70% confluence and lysed in complete RIPA buffer (Sigma, R0278) for 30 min at 4°C. Lysates were centrifuged at 16000*g* for 30 min before the supernatant was removed and sonicated. 15 µg of cell lysate was run on a 4-15% PROTEAN TGX gel (BIORAD, 456,1083) and transferred using the TransBlot-Turbo transfer system (BIORAD). Lysates were subjected to western blotting with the Bio-Rad Western blot system. Membranes were blocked with 5% milk for 1 h before incubation with primary and secondary antibodies.

Bioconjugation. Conjugation of A5/158 and isotype control antibodies to saporin, was carried out using a streptavidin-biotin conjugation technique previously described (28).

Conjugation of A5/158 and isotype control antibodies to monomethyl auristatin E (MMAE) was carried out by Abzena (Cambridge) Ltd. A5/158 antibody in PBS pH 7.5, 5 mM EDTA (20.7 mg, 1.0 eq.) was reduced by adding 5 mM tris(2-carboxyethyl)phosphine (TCEP, 5.0 eq.). The reduction was allowed to proceed at 40°C for 2 h with a final antibody concentration of 5 mg/mL. The reduction mixture was allowed to cool to 22°C and a 10 mM solution of mc-vc-PAB-MMAE in DMSO (380 µL, 9.0 eq.) was added (final concentration of 10% DMSO and antibody concentration of 4.0 mg/mL). The conjugation reaction was allowed to proceed at 22°C for 2 h. The conjugate was purified by ultrafiltration/diafiltration (UF/DF) using a Vivaspin 20 (30 kDa MWCO) and buffer exchanged into PBS.

Isotype antibody in PBS pH 7.5, 5 mM EDTA (20 mg, 1.0 eq.) was reduced as described above. A 7.6 mM solution of mc-vc-PAB-MMAE in DMSO (105 µL, 6.0 eq.)

was added to the reduced antibody (final concentration of 10% DMSO and antibody concentration of 4.0 mg/mL). The conjugation reaction and antibody purification was as described above.

To determine the drug to antibody ratio (DAR) the ADCs were analyzed by hydrophobic interaction chromatography (HIC) using a Tosoh TSKgel Butyl-NPR column. The resulting ADCs had a DAR of 4.0 and 3.4 for A5/158-vc-MMAE and Isotype-vc-MMAE, respectively. Aggregation of conjugates was determined by size exclusion chromatography (SEC) using a Waters BEH 200 Å column.

ADC cell proliferation/viability assays. 1 x 10^3 – 2 x 10^3 cells/well were seeded into a 96-well plate. After 48 h cells were treated with antibodies/ADCs. Cell growth was tracked and quantified by the Live-Cell Analysis System IncuCyte (EssenBioscience). At end point, cell viability was quantified by CellTiter-Glo (Promega).

In vivo studies

All animal work was carried out under UK Home Office Project license P6AB1448A (Establishment License, X702B0E74) which outlines experimental protocols and endpoints. Work was approved by the Animal Welfare and Ethical Review Body at the ICR. 6-7 week old female NOD.Cg-*Prkdc*^{scid} *Il2rg*^{tm1Wjl}/SzJ (NSG) mice were purchased from Charles River. Animals were housed in IVC type cages which are run under negative air flow. Mice had food and water ad libitum and were monitored daily by the ICR Biological Services Unit staff.

Subcutaneous inoculation. 1 x 10^6 MG-63-mChLuc2 cells were injected subcutaneously into the flank under general anesthesia. Tumor growth was measured 3 times a week using calipers. Tumor volumes and growth rates were calculated as described previously (12).

ADC treatment. Antibodies and ADCs were diluted in PBS immediately prior to administration. Vehicle (PBS) or 10 mg/kg of A5/158, Isotype-vc-MMAE or A5/158-vc-MMAE were administered into the lateral tail vein of mice twice a week for two weeks. Primary tumors were weighed at necropsy.

IVIS imaging. Mice were injected intraperitoneally with 150 mg/kg D-luciferin (Caliper Life Sciences) and after 5 min mice were imaged *in vivo* using an IVIS imaging chamber (IVIS Illumina II). Organs were also imaged individually *ex vivo*. Luminescence measurements (photons/second/cm^2) were acquired over 1-60 sec and analyzed using the Living Image software (PerkinElmer) using a constant sized region of interest over the tissues.

Immunohistochemistry. Mouse tumors and organs were harvested at necropsy, formalin-fixed and paraffin-embedded. Tumor sections were stained with human Endo180 mAb 39.10 as described above for TMA staining. For lungs and livers, 3 sections approximately 150 μm apart were stained for human lamin A/C. Images of stained sections were acquired on the NanoZoomer Digital Pathology (Hamamatsu). Quantification of the number and size of lamin A/C-positive lesions in lungs and livers was carried out using QuPath v0.3.0 (RRID:SCR_018257) (29). Briefly, a pixel classifier was trained for lamin A/C-positive cell recognition using the artificial neural network algorithm. Annotations were drawn around whole tissue sections which were divided into tiles using SLIC superpixel segmentation. Identified by the trained pixel classifier, tumor lesions were quantified by converting tiles to annotations. Metastatic lesions were defined as > 1500 μm^2 (approximately >10 tumor cells).

Real-time quantitative polymerase chain reaction (RT-qPCR). Tumor tissue was harvested at necropsy and snap frozen in liquid nitrogen. Tumor tissue was

homogenized in Precellys Lysing Kit tubes (P000911-LYSK0-A) containing RLT buffer (QIAGEN) plus 1:100 β-mercaptoethanol. RNA was isolated using the RNeasy Mini Kit (QIAGEN, 74104) and cDNA was generated using the Superscript kit (Invitrogen, 18091050) according to the manufacturer's instructions. RT-qPCR was performed using Taqman Gene Expression Assay Probes (Life Technologies; UBC probe, Hs00824723_m1; MRC2, Hs00977846_m1) on a QuantStudio 6 Flex Real Time PCR system (Applied Biosystems) and relative quantification was performed using QuantStudio Real-Time PCR software. Each reaction was performed in triplicate. Relative *MRC2* expression levels were normalized to *UBC*.

Statistics

Statistics were performed using GraphPad Prism 9 (RRID:SCR_002798). Data was normality tested before one-way ANOVA analysis was performed with Tukey test for multiple comparison of parametric data, or Kruskal-Wallis test was performed with Dunn's multiple comparison test for non-parametric data. Non-significant (ns) p values > 0.05.

Data availability

Series matrix files of whole transcript expression data from STS tumors and control normal fat specimens were downloaded from the Gene Expression Omnibus (GEO) site: GSE21122 (RRID:SCR_005012) (30). Gene expression of *MRC2* from the Innovative Therapies for Children with Cancer (ITCC) and The Cancer Genome Atlas (TCGA) datasets was retrieved using the R2: Genomics Analysis and Visualization Platform [http://r2.amc.nl] and [http://r2platform.com]. *MRC2* gene expression from Cancer Cell Line Encyclopedia (CCLE) datasets was retrieved from [https://depmap.org/portal/] (RRID:SCR_017655). Expression of *MRC2* in pediatric sarcoma and normal tissue was retrieved from the National Cancer Institute (NCI) OncoGenomics data portal [https://clinomics.ccr.cancer.gov/clinomics/public/].

Results

Endo180 is expressed on multiple sarcoma subtypes

Endo180 protein expression was assessed by immunohistochemistry using the anti-Endo180 mAb 39.10 (Fig. 1a) in rhabdomyosarcoma, liposarcoma, leiomyosarcoma, synovial sarcoma, fibrosarcoma and undifferentiated pleomorphic sarcoma (UPS) TMAs (Fig. 1b,c; Supplementary Fig. S1). We have previously reported the specificity of the 39.10 antibody (24). High levels of Endo180 protein are detected in the majority of STS - 64.0% of rhabdomyosarcomas (126/197), 38.5% well-differentiated liposarcomas (20/52), 93.1% de-differentiated liposarcomas (54/58), 64.2% leiomyosarcomas (97/151), 76.1% synovial sarcomas (32/42), 87.5% fibrosarcomas (21/24) and 64.3% of UPS (65/101) (Fig. 1c). Examples of cores scored positive and negative are provided in Supplementary Fig. S1. Of note, due to its constitutive recycling properties, Endo180 staining is frequently observed in the perinuclear region characteristic of clustered intracellular endosomes (11). In samples with Endo180-negative tumor cells, Endo180-positive CAFs are frequently detected in the tumor stroma (Supplementary Fig. S1). Fibroblasts with low level Endo180 expression are detected in normal human tissue controls (Supplementary Fig. S2a).

Equivalent findings were obtained by examining *MRC2* (Endo180) gene expression in STS of different subtypes from Barretina and colleagues (30), with *MRC2* highly expressed in the majority of adult STS compared to normal fat (Fig. 1d). A similar profile is seen in the STS samples from the TCGA database (Supplementary Fig. S2b). Within pediatric datasets, comparison of cancer samples and normal tissue from the NCI OncoGenomics database (Supplementary Fig. S2c) also demonstrates higher *MRC2* expression in the majority of sarcoma samples compared to the mean normal tissue expression (Supplementary Fig. S2c), with notable elevation of *MRC2* expression in osteosarcomas. An equivalent expression pattern has been reported in

samples from the St Jude PeCan Data Portal (21). Finally, gene expression in rhabdomyosarcomas from the Innovative Therapies for Children with Cancer (ITCC) datasets (Fig. 1e) show increased *MRC2* expression compared to normal skeletal muscle. There is no significant difference between the rhabdomyosarcoma subtypes, categorized by fusion status of forkhead (*FKHR*) to paired box 3 (*PAX3*) or PAX 7. Together, immunohistochemical staining and bioinformatic analysis demonstrates expression of Endo180 in sarcomas and CAFs is elevated compared to normal tissue fibroblasts, indicating that on-target, off-tumor toxicities would be limited in patients.

A5/158 recognizes Endo180 expressed on sarcoma cell lines

Analysis of expression data from Cancer Cell Line Encyclopedia (CCLE) is consistent with the immunohistochemistry staining and gene expression analysis of primary tumors (Fig. 1; Supplementary Fig. S1) showing significantly higher *MRC2* expression in both STS and bone sarcoma cell lines compared to breast or colorectal cancer cell lines (Fig. 2a). To evaluate if the anti-Endo180 mAb A5/158, which recognizes an epitope in CTLD2 (31) (Fig. 1a), is a suitable candidate for development into an ADC, we assessed its binding specificity in multiple sarcoma cell lines. Sarcoma cell lines: MG-63 (osteosarcoma), HT-1080 (fibrosarcoma), A-204 (malignant rhabdoid tumor), SJSA-1 (osteosarcoma), SK-UT-1 (uterine leiomyosarcoma) and G-402 (leiomyoblastoma), along with the known Endo180-negative epithelial cell lines HT-29 (colorectal cancer) and MCF-7 (breast cancer) were subject to western blotting with A5/158 or an isotype control antibody (Fig. 2b). As previously reported (23,24), Endo180 protein is not detected in either epithelial cancer cell line and, consistent with the CCLE data (Fig. 2a), the majority of sarcoma cell lines show Endo180 protein expression detected by A5/158 but not isotype control antibody (Fig. 2b). Lower Endo180 protein levels in the SK-UT-1 and G-402 cell lines reflects lower *MRC2* expression in the CCLE dataset compared to the other sarcoma cell lines.

In immunofluorescence staining of permeabilized cells in culture using A5/158 directly conjugated to an Alexa Fluor 488 dye (A5/158-488), both the MG-63 and HT-1080 sarcoma cell lines show intracellular vesicular staining, clustered in the perinuclear region (Fig. 2c) and mirroring the staining pattern in the STS TMAs (Fig. 1b; Supplementary Fig. S1). In contrast, no staining is detected in the MCF-7 breast cancer cells or with the isotype control antibody. Examining a broader range of sarcoma cell lines (Supplementary Fig. S3a), levels of immunofluorescence staining concur with the CCLE expression (Fig. 2a) and Western blotting (Fig. 2b) data and additionally demonstrate that Endo180 expression is homogenous in the majority of cell lines, with only slight heterogeneity in staining intensity seen in SK-UT-1 and G-402 lines.

A5/158 is suitable for intracellular drug delivery

Endo180 is known to be rapidly and constitutively internalized into endosomes where ligand detaches in the low pH environment and is trafficked to the lysosomes for degradation, while the receptor is recycled back to the plasma membrane (10,11,23). To assess whether the internalizing receptor can deliver an intact antibody intracellularly, A5/158-488 or Isotype-488 were incubated with unfixed Endo180-positive MG-63 and HT-1080, and Endo180-negative MCF-7 cells for 1 h at 4^{o}C before unbound antibody was removed by washing and coverslips were incubated with the lysosomal marker LysoTracker Red and Hoechst nuclear stain for a further 30 min at 37^{o}C. Strong punctate fluorescence in the green channel is detected in MG-63 and HT-1080 sarcoma cells (Fig. 3a, left panel) demonstrating A5/158 has been internalized. No A5/158-488 fluorescence is detected in the MCF-7 cells. Additionally, no fluorescence is detected with the Isotype-488 antibody (Supplementary Fig. S3b). Merged images of internalized A5/158-488 and the LysoTracker highlight areas of co-localization, indicating that A5/158 is trafficked to the lysosomes (Fig. 3a, right panel).

To confirm that internalized antibodies are capable of delivering a cytotoxic drug intracellularly, A5/158 was conjugated to the ribosome inactivating toxin, saporin, using a streptavidin-biotin (sb) rapid conjugation technique (28). MG-63, HT-1080 and MCF-7 cells incubated with unconjugated A5/158 have no impairment in cell growth or cell viability, determined at endpoint by CellTiter-Glo (Fig. 3b,c). Saporin is not membrane permeable and therefore not able to cause cell cytotoxicity alone. However, when conjugated to A5/158, MG-63 and HT-1080 cell growth and cell viability is significantly impaired. As saporin is conjugated via a non-cleavable linker, these data indicate that A5/158-sb-Saporin is internalized into Endo180 expressing cells, trafficked to the lysosome for degradation and the toxin released intracellularly. This effect is not seen in MCF-7 cells or with Isotype-sb-Saporin conjugate treatment demonstrating that inhibition of cell growth and viability is dependent on Endo180-mediated A5/158-sb-Saporin internalization.

Endo180 expressing cell lines are sensitive to A5/158-vc-MMAE

Next, an ADC was created by conjugating A5/158 to the microtubule targeting drug monomethyl auristatin E (MMAE) via a dipeptide valine-citrulline linker (vc) which, upon internalization, is cleaved by lysosomal cathepsin enzymes (Fig. 4a). This linker-payload combination was selected as it is utilized by 4 of the 11 currently FDA-approved ADCs, and in 5 out of the 12 ADCs being developed for the treatment of sarcoma (8). In addition, the membrane permeability of MMAE can cause a desirable bystander killing effect on the surrounding cells. The isotype control antibody was conjugated to the same linker-payload combination, and the resulting ADCs termed A5/158-vc-MMAE and Isotype-vc-MMAE. Hydrophobic interaction chromatography was used to determine the composition of the drug to antibody ratios (DAR) for each ADC (Supplementary Fig. S4a). The average DAR achieved was 4.0 and 3.4 for A5/158-vc-MMAE and Isotype-vc-MMAE, respectively, comparable to the average DAR of 3.5 of the ADC Trastuzumab-DM1 which is approved for the treatment of

HER2-positive breast cancers. Conjugation of A5/158 to MMAE does not increase antibody aggregation, assessed by size exclusion chromatography (Supplementary Fig. S4b), nor disrupt its ability to bind Endo180, assessed by Western blotting (Supplementary Fig. S4c).

To examine the efficacy of A5/158-vc-MMAE *in vitro*, increasing concentrations of A5/158-vc-MMAE and Isotype-vc-MMAE were incubated with Endo180-positive sarcoma (MG-63, HT-1080, A-204), Endo180-low sarcoma (G-402, SK-UT-1) and Endo180-negative (MCF-7, HT-29) control cell lines (Fig. 4b). Endo180-positive cell lines are sensitive to A5/158-vc-MMAE whilst Endo180-negative cell lines are comparatively resistant. Although to a lesser extent than Endo180-positive cell lines, Endo180-low cell lines still show a specific decrease in viability when treated with A5/158-vc-MMAE, demonstrating a correlation between Endo180 expression and sensitivity to A5/158-vc-MMAE.

A5/158-vc-MMAE decreases sarcoma tumor growth and metastasis

As MG-63 cells show sensitivity to A5/158-vc-MMAE *in vitro* (Fig. 4b) a sarcoma tumor model using these cells was established subcutaneously in immunodeficient NSG mice to assess efficacy *in vivo*. In a pilot tolerability experiment (Supplementary Fig. S5a), mice were treated with 2.5, 5 and 10 mg/kg A5/158-vc-MMAE or vehicle (PBS) when MG-63-mChLuc2 tumors were ~3.5 mm in diameter (day 10). Alternatively, two mice were treated with vehicle until tumors were ~8.5 mm in diameter (day 24) and then treated with two doses of 5 mg/kg A5/158-vc-MMAE. The pilot experiment was terminated on day 32 due to the development of large lymph node metastases in the vehicle-treated mice. No mice treated with A5/158-vc-MMAE showed any clinical signs of distress or weight loss, indicating that the ADC does not cause dose limiting toxicities (Supplementary Fig. S5b). A dose dependent inhibition of tumor growth is observed in mice treated with A5/158-vc-MMAE, with almost complete tumor regression in the

mouse treated with 4 doses 10 mg/kg of A5/158-vc-MMAE (Supplementary Fig. S5c-f). 39.10 staining of tumors at necropsy indicates that surviving tumor cells retain Endo180 expression *in vivo*, indicating that tumors would be sensitive to further ADC treatment (Supplementary Fig. S5f). Examination of organs at necropsy and immunohistochemical staining of human lamin A/C used to identify MG-63 tumor cells, demonstrates all concentrations of A5/158-vc-MMAE, including 5 mg/kg treatment starting at day 24, impairs metastatic colonization of the lungs and liver (Supplementary Fig. S6).

Based on the pilot tolerability study, NSG mice were inoculated subcutaneously with $1x10^6$ MG-63-mChLuc2 cells. Once the tumors had reached ~3 mm in diameter, mice were administered intravenously with vehicle (PBS), A5/158 alone, A5/158-vc-MMAE or Isotype-vc-MMAE (all 10 mg/kg) twice weekly for a total of four doses (Fig. 5a). No toxicity is observed from any treatment either through monitoring animal bodyweight (Fig. 5b) or clinical signs of distress. No effect on tumor growth rate nor final tumor size or weight is observed with A5/158 alone or Isotype-vc-MMAE treatment compared to vehicle treated mice. By contrast, treatment with A5/158-vc-MMAE results in tumor regression (Fig. 5c-f). In line with the pilot tolerability study (Supplementary Fig. S5f), the surviving cells in the A5/158-vc-MMAE treated MG-63 tumors retain Endo180 expression as monitored by immunohistochemistry and RT-qPCR (Fig. 5g,h).

Ex vivo IVIS imaging of the lungs of the animals from Fig. 5 shows a significant reduction in bioluminescent signal in the lungs of A5/158-vc-MMAE-treated mice compared to control mice (Fig. 6a). Human lamin A/C staining reveals a substantial reduction in both the number and size of lung metastases in A5/158-vc-MMAE treated mice (Fig. 6b,c). Similarly, 8 of 11 control mice developed liver metastases in contrast to 0 of 5 mice treated with A5/158-vc-MMAE (Fig. 6d; Supplementary Fig. S7). Finally, 9 of 11 control mice, but only 1 of 5 A5/158-vc-MMAE treated mice, developed overt

lymph node metastases (Fig. 6e). Taken together, these data demonstrate that treatment of MG-63 tumor-bearing mice with A5/158-vc-MMAE effectively induces primary tumor regression and inhibits the outgrowth of metastatic lesions in the lung, liver and lymph nodes.

Discussion

At the time of writing, there are 11 FDA approved ADCs available in the clinic, 7 of which have only been approved since 2018 making ADCs one of the most rapidly growing fields of cancer therapeutics. Owing to the variable responses of sarcoma tumors to first line therapies, research into the development of personalized medicines has increased. Approaches have included targeting antigens expressed on sarcomas with ADCs, such leucine-rich repeat containing 15 (LRRC15) (32), glycoprotein non-metastatic b protein (GPNMB) (33) and neural cell adhesion molecule (NCAM, CD56) (34) plus a membrane type 1-matrix metalloproteinase (MT1-MMP) bicycle toxin conjugate (21). In total, 9 immunoconjugates targeting sarcoma have entered clinical trials (8). Despite these advancements, no antibody-based therapies have yet been approved for sarcoma treatment and therefore, there remains a significant unmet clinical need for patients, especially in metastatic settings.

Here we report the first *in vivo* assessment of an Endo180 (*MRC2*)-directed ADC targeting in sarcoma. High levels of Endo180 protein has been reported previously in osteosarcomas (17,19,21), with Endo180 identified as one of the most upregulated genes in proteomic profiling, transcriptomic analysis and immunohistochemical staining of osteosarcoma patient samples and cell lines, compared to normal tissues and other pediatric cancers (21). Despite this, Endo180 expression in the broader range of sarcoma subtypes has not been investigated. In this study we assessed Endo180 protein levels in 625 STS clinical samples and complemented this with bioinformatics analysis of sarcoma gene expression datasets. Strikingly, high levels of

Endo180 protein are detected in the majority (415 out of 625) of the common STS subtype tumors. A similar picture emerges assessing *MRC2* expression in sarcoma gene expression profiling datasets, highlighting the potential of Endo180 as a therapeutic target.

In this study we show that an A5/158-vc-MMAE ADC specifically kills Endo180 expressing sarcoma cells lines. This is in agreement with a previous study showing that an alternative Endo180 mAb vc-MMAE conjugate reduced viability of Endo180-positive sarcoma cell lines *in vitro* and had efficacy against an Endo180-positive human myeloid leukemia xenograft (19). Similarly, it has been demonstrated recently that Endo180 expression is upregulated on malignant mesotheliomas and that an Endo180-targeting ADC causes cytotoxicity of mesothelioma cell lines *in vitro* (16).

Previously, we demonstrated that an anti-Endo180 ^{125}I-Fab' fragment is rapidly internalized from the cell surface and that ~70% of internalized Fab' is degraded intracellularly without affecting the half-life of Endo180 receptor, as measured in a ^{35}S-methionine pulse chase assay (23). This early study provided two important pieces of information. First, that an Endo180-targeting ADC would be able to release its cytotoxic payload intracellularly and indeed, as demonstrated here, the A5/158-vc-MMAE is trafficked into the lysosomes for degradation. Second, that the target receptor would remain present on any cell surviving an initial encounter with the ADC, as observed in Fig. 5g,h, and hence would be sensitive to further rounds of treatment. This is important as development of resistance to ADCs utilizing the vc-MMAE linker-payload complex has been observed and attributed to the downregulation of the target receptor and/or removal of MMAE by the efflux pump multidrug resistance protein 1 (MDR1) (35-37). Approaches such as modification of the ADC linker, conjugation with drugs which are not MDR1 substrates, or engineering

dual-drug ADCs have been developed to maintain efficacy in MDR1-expressing tumors (37-39). Consequently, should resistance to MMAE occur via MDR1-mediated efflux, such modified ADCs could restore anti-tumor activity as retention of Endo180 expression would ensure that a second ADC is still efficiently internalized.

The first limitation of this study, and previous Endo180 ADC studies (16,19), is the use of an ADC specific for human Endo180 requiring human tumors to be grown in immunodeficient mice. This precludes an assessment of on-target off-tumor toxicities and immune engagement. In the model used here, no adverse effects were seen in the body weight or other signs of ill-health in the mice treated with either the A5/158-vc-MMAE or Isotype-vc-MMAE ADCs, demonstrating the stability of the ADC in the circulation and the absence of off-target toxicities. Although the Endo180 knockout mouse has no discernible abnormalities, Endo180 is expressed in normal tissue fibroblasts, albeit at lower level than in sarcomas (Fig. 1; Supplementary Fig. S1 and Fig. S2). Consequently, further studies are required to determine if there are any on-target, off-tumor toxicities associated with this therapy. Immune recruitment by antibodies has been implicated with anti-tumor efficacy via antibody-dependent cellular cytotoxicity (ADCC) and antibody-dependent cellular phagocytosis (ADCP) carried out by natural killer and macrophage cells, respectively. This ADCC effect has been attributed to the HER2-targeting antibody, trastuzumab, in pre-clinical models and likely contributes to the efficacy of the corresponding ADC, trastuzumab-DM1 (T-DM1) (40-42), although this would not be evident in an immunodeficient setting. Finally, in addition to expression on the sarcoma tumor cells, Endo180 levels are also elevated in CAFs compared to normal tissue fibroblasts (13). Due to the species specificity of A5/158-vc-MMAE, the effects of targeting both Endo180-positive human tumor cells and mouse CAFs could not be assessed. The development of an ADC recognizing mouse Endo180 will be required to perform a full pre-clinical assessment of any normal tissue toxicity, to examine the immune engagement of the ADC which could enhance

the anti-tumor effect of the therapy at both the primary and metastatic sites and to determine the benefit of targeting both tumor cells and stromal CAFs.

The second limitation of this study is the potency of the A5/158-vc-MMAE ADC, which has an IC_{50} in Endo180 expressing cells of ~5 µg/mL, make it less effective that other ADCs with an MMAE payload (19,43,44). However, in these other studies it is notable that the control ADCs were substantially more cytotoxic likely reflecting differences in target cell density and/or assay duration. Nonetheless, the A5/158 ADC requires further optimization to improve its efficacy prior to further clinical development. Whilst higher drug to antibody ratios can increase the cytotoxicity of an ADC, it will also be particularly important to investigate the efficacy and optimal dosing/scheduling of A5/158 conjugated to alternative payloads such as SN-38, duocarmycin, pyrrolobenzodiazepine (PBD) dimers and exatecan, which have been used in the development of more recent ADCs against sarcomas and other tumor types (45-49). Additionally, in mice treated with A5/158-vc-MMAE, not all Endo180 positive MG-63 tumor cells were depleted (Fig. 5g,h) and although this may reflect the ADC potency, lack penetration of the ADC into the tumor may also play a role. The use of an antibody fragment or alternative scaffold drug conjugates may improve tumor penetration owing their smaller size; however these small format drug conjugates are often associated with more rapid clearance and therefore the duration of treatment can be limited (50).

In summary, the A5/158-vc-MMAE ADC specifically kills Endo180 expressing cell lines, causes regression of an Endo180-positive osteosarcoma tumor model and reduces metastatic colonization of the lung, liver and lymph nodes. This identifies Endo180 as a promising pharmacological target for the treatment of sarcoma, particularly of metastatic sarcomas for which there are currently no specific and effective therapies.

Author contributions

Conceptualization RJE, CMI

Supervision DWP, KS, CMI

Funding acquisition JMS, CMI

Investigation RJE, DWP, JS, AK, GPB, JMS, KS, CMI

Writing - original draft RJE, KS, CMI

Writing - review and editing RJE, DWP, JS, AK, GPB, JMS, KS, CMI

Acknowledgements

This study was funded by a Cancer Research UK PhD Studentship (RJE) and Program Grants from Breast Cancer Now (CMI) as part of Program Funding to the Breast Cancer Now Toby Robins Research Centre. KS is supported by an EMBO fellowship, ALTF 799-2020. JMS was supported by generous funds from the Chris Lucas Trust and the Talan's Trust. This work represents independent research supported by the National Institute for Health Research (NIHR) Biomedical Research Centre at The Royal Marsden NHS Foundation Trust and the Institute of Cancer Research, London. The views expressed are those of the authors and not necessarily those of the NIHR or the Department of Health and Social Care.

We thank Nicolas Camper (Abzena (Cambridge) Ltd) for managerial oversight of the ADC production, and Sophia Karagiannis and Melina Hoffmann at the Breast Cancer Now Unit, King's College London for sharing their expertise throughout this project and particularly for their help with the saporin conjugation. We thank Khin Thway, Anastasia Constantinidou and Reem Al-Saadi for collection and/or preparation of fixed sarcoma tissues, Paul Huang (ICR) for sharing sarcoma cell lines, Naomi Guppy and her team in the Breast Cancer Now Toby Robins Research Centre Nina Barough Pathology Core Facility for antibody optimization and pathology support, and the ICR Biological Services Unit and the FACS and Light Microscopy Facility for their expert help.

References

1. WHO. World Health Organization classification of soft tissue and bone tumours. IARC Press: Lyon, France. 5th edition ed2020.
2. Taylor BS, Barretina J, Maki RG, Antonescu CR, Singer S, Ladanyi M. Advances in sarcoma genomics and new therapeutic targets. *Nature Reviews Cancer* 2011;**11**(8):541-57 doi 10.1038/nrc3087.
3. Miller RW, L Young Jr. J, Novakovic B. Childhood cancer. *Cancer* 1995;**75**(S1):395-405 doi https://doi.org/10.1002/1097-0142(19950101)75:1+<395::AID-CNCR2820751321>3.0.CO;2-W.
4. Helman LJ, Meltzer P. Mechanisms of sarcoma development. *Nature Reviews Cancer* 2003;**3**(9):685-94 doi 10.1038/nrc1168.
5. Tap WD, Wagner AJ, Schoffski P, Martin-Broto J, Krarup-Hansen A, Ganjoo KN*, et al.* Effect of Doxorubicin Plus Olaratumab vs Doxorubicin Plus Placebo on Survival in Patients With Advanced Soft Tissue Sarcomas: The ANNOUNCE Randomized Clinical Trial. *JAMA* 2020;**323**(13):1266-76 doi 10.1001/jama.2020.1707.
6. Bielack S, Carrle D, Casali PG, Group EGW. Osteosarcoma: ESMO clinical recommendations for diagnosis, treatment and follow-up. *Ann Oncol* 2009;**20 Suppl 4**:137-9 doi 10.1093/annonc/mdp154.
7. Duchman KR, Gao Y, Miller BJ. Prognostic factors for survival in patients with high-grade osteosarcoma using the Surveillance, Epidemiology, and End Results (SEER) Program database. *Cancer Epidemiol* 2015;**39**(4):593-9 doi 10.1016/j.canep.2015.05.001.
8. Polito L, Calafato G, Bortolotti M, Chiarelli Olivari C, Maiello S, Bolognesi A. Antibody Conjugates for Sarcoma Therapy: How Far along Are We? *Biomedicines* 2021;**9**(8):978.

9. Kjøller L, Engelholm LH, Høyer-Hansen M, Danø K, Bugge TH, Behrendt N. uPARAP/endo180 directs lysosomal delivery and degradation of collagen IV. *Experimental cell research* 2004;**293**(1):106-16.

10. Wienke D, MacFadyen JR, Isacke CM. Identification and characterization of the endocytic transmembrane glycoprotein Endo180 as a novel collagen receptor. *Mol Biol Cell* 2003;**14**(9):3592-604 doi 10.1091/mbc.e02-12-0814.

11. Howard MJ, Isacke CM. The C-type lectin receptor Endo180 displays internalization and recycling properties distinct from other members of the mannose receptor family. *J Biol Chem* 2002;**277**(35):32320-31 doi 10.1074/jbc.M203631200.

12. Jenkins L, Jungwirth U, Avgustinova A, Iravani M, Mills AP, Haider S*, et al.* Cancer-associated fibroblasts suppress CD8+ T cell infiltration and confer resistance to immune checkpoint blockade. *Cancer Res* 2022 doi 10.1158/0008-5472.CAN-21-4141.

13. Jungwirth U, van Weverwijk A, Evans RJ, Jenkins L, Vicente D, Alexander J*, et al.* Impairment of a distinct cancer-associated fibroblast population limits tumour growth and metastasis. *Nature Communications* 2021;**12**(1):3516 doi 10.1038/s41467-021-23583-1.

14. East L, McCarthy A, Wienke D, Sturge J, Ashworth A, Isacke CM. A targeted deletion in the endocytic receptor gene Endo180 results in a defect in collagen uptake. *EMBO reports* 2003;**4**(7):710-6.

15. Engelholm LH, List K, Netzel-Arnett S, Cukierman E, Mitola DJ, Aaronson H*, et al.* uPARAP/Endo180 is essential for cellular uptake of collagen and promotes fibroblast collagen adhesion. *The Journal of cell biology* 2003;**160**(7):1009-15.

16. Cakilkaya P, Sorensen RR, Jurgensen HJ, Krigslund O, Gardsvoll H, Nielsen CF*, et al.* The Collagen Receptor uPARAP in Malignant Mesothelioma: A

Potential Diagnostic Marker and Therapeutic Target. *Int J Mol Sci* 2021;**22**(21) doi 10.3390/ijms222111452.

17. Engelholm LH, Melander MC, Hald A, Persson M, Madsen DH, Jürgensen HJ*, et al.* Targeting a novel bone degradation pathway in primary bone cancer by inactivation of the collagen receptor uPARAP/Endo180. *The Journal of Pathology* 2016;**238**(1):120-33 doi https://doi.org/10.1002/path.4661.

18. Huijbers IJ, Iravani M, Popov S, Robertson D, Al-Sarraj S, Jones C*, et al.* A role for fibrillar collagen deposition and the collagen internalization receptor endo180 in glioma invasion. *PLoS One* 2010;**5**(3):e9808 doi 10.1371/journal.pone.0009808.

19. Nielsen CF, van Putten SM, Lund IK, Melander MC, Nørregaard KS, Jürgensen HJ*, et al.* The collagen receptor uPARAP/Endo180 as a novel target for antibody-drug conjugate mediated treatment of mesenchymal and leukemic cancers. *Oncotarget* 2017;**8**(27):44605-24 doi 10.18632/oncotarget.17883.

20. Takahashi S, Yamada-Okabe H, Hamada K, Ohta S, Kawase T, Yoshida K*, et al.* Downregulation of uPARAP mediates cytoskeletal rearrangements and decreases invasion and migration properties in glioma cells. *J Neurooncol* 2011;**103**(2):267-76 doi 10.1007/s11060-010-0398-z.

21. Wang Y, Tian X, Zhang W, Zhang Z, Lazcano R, Hingorani P*, et al.* Comprehensive Surfaceome Profiling to Identify and Validate Novel Cell-Surface Targets in Osteosarcoma. *Mol Cancer Ther* 2022;**21**(6):903-13 doi 10.1158/1535-7163.MCT-21-0836.

22. Chari RV, Martell BA, Gross JL, Cook SB, Shah SA, Blättler WA*, et al.* Immunoconjugates containing novel maytansinoids: promising anticancer drugs. *Cancer Res* 1992;**52**(1):127-31.

23. Isacke CM, van der Geer P, Hunter T, Trowbridge IS. p180, a novel recycling transmembrane glycoprotein with restricted cell type expression. *Mol Cell Biol* 1990;**10**(6):2606-18 doi 10.1128/mcb.10.6.2606-2618.1990.

24. Wienke D, Davies GC, Johnson DA, Sturge J, Lambros MB, Savage K*, et al.* The collagen receptor Endo180 (CD280) Is expressed on basal-like breast tumor cells and promotes tumor growth in vivo. *Cancer Res* 2007;**67**(21):10230-40 doi 10.1158/0008-5472.Can-06-3496.

25. Kononen J, Bubendorf L, Kallioniemi A, Barlund M, Schraml P, Leighton S*, et al.* Tissue microarrays for high-throughput molecular profiling of tumor specimens. *Nat Med* 1998;**4**(7):844-7 doi 10.1038/nm0798-844.

26. Thway K, Robertson D, Jones RL, Selfe J, Shipley J, Fisher C*, et al.* Endosialin expression in soft tissue sarcoma as a potential marker of undifferentiated mesenchymal cells. *Br J Cancer* 2016;**115**(4):473-9 doi 10.1038/bjc.2016.214.

27. Wachtel M, Runge T, Leuschner I, Stegmaier S, Koscielniak E, Treuner J*, et al.* Subtype and Prognostic Classification of Rhabdomyosarcoma by Immunohistochemistry. *Journal of Clinical Oncology* 2006;**24**(5):816-22 doi 10.1200/jco.2005.03.4934.

28. Hoffmann RM, Mele S, Cheung A, Larcombe-Young D, Bucaite G, Sachouli E*, et al.* Rapid conjugation of antibodies to toxins to select candidates for the development of anticancer Antibody-Drug Conjugates (ADCs). *Scientific Reports* 2020;**10**(1):8869 doi 10.1038/s41598-020-65860-x.

29. Bankhead P, Loughrey MB, Fernandez JA, Dombrowski Y, McArt DG, Dunne PD*, et al.* QuPath: Open source software for digital pathology image analysis. *Sci Rep* 2017;**7**(1):16878 doi 10.1038/s41598-017-17204-5.

30. Barretina J, Taylor BS, Banerji S, Ramos AH, Lagos-Quintana M, DeCarolis PL*, et al.* Subtype-specific genomic alterations define new targets for soft-tissue sarcoma therapy. *Nature Genetics* 2010;**42**(8):715-21 doi 10.1038/ng.619.

31. Sturge J, Wienke D, East L, Jones GE, Isacke CM. GPI-anchored uPAR requires Endo180 for rapid directional sensing during chemotaxis. *The Journal of cell biology* 2003;**162**(5):789-94 doi 10.1083/jcb.200302124.

32. Purcell JW, Tanlimco SG, Hickson J, Fox M, Sho M, Durkin L*, et al.* LRRC15 Is a Novel Mesenchymal Protein and Stromal Target for Antibody–Drug Conjugates. *Cancer Research* 2018;**78**(14):4059-72 doi 10.1158/0008-5472.Can-18-0327.

33. Roth M, Barris DM, Piperdi S, Kuo V, Everts S, Geller D*, et al.* Targeting Glycoprotein NMB With Antibody-Drug Conjugate, Glembatumumab Vedotin, for the Treatment of Osteosarcoma. *Pediatr Blood Cancer* 2016;**63**(1):32-8 doi 10.1002/pbc.25688.

34. Wood AC, Maris JM, Gorlick R, Kolb EA, Keir ST, Reynolds CP*, et al.* Initial testing (Stage 1) of the antibody-maytansinoid conjugate, IMGN901 (Lorvotuzumab mertansine), by the pediatric preclinical testing program. *Pediatr Blood Cancer* 2013;**60**(11):1860-7 doi 10.1002/pbc.24647.

35. Loganzo F, Tan X, Sung M, Jin G, Myers JS, Melamud E*, et al.* Tumor Cells Chronically Treated with a Trastuzumab–Maytansinoid Antibody–Drug Conjugate Develop Varied Resistance Mechanisms but Respond to Alternate Treatments. *Molecular Cancer Therapeutics* 2015;**14**(4):952-63 doi 10.1158/1535-7163.Mct-14-0862.

36. Rexer BN, Arteaga CL. Intrinsic and acquired resistance to HER2-targeted therapies in HER2 gene-amplified breast cancer: mechanisms and clinical implications. *Crit Rev Oncog* 2012;**17**(1):1-16 doi 10.1615/critrevoncog.v17.i1.20.

37. Yu S-F, Zheng B, Go M, Lau J, Spencer S, Raab H*, et al.* A Novel Anti-CD22 Anthracycline-Based Antibody–Drug Conjugate (ADC) That Overcomes Resistance to Auristatin-Based ADCs. *Clinical Cancer Research* 2015;**21**(14):3298-306 doi 10.1158/1078-0432.Ccr-14-2035.

38. Kovtun YV, Audette CA, Mayo MF, Jones GE, Doherty H, Maloney EK*, et al.* Antibody-maytansinoid conjugates designed to bypass multidrug resistance. *Cancer Res* 2010;**70**(6):2528-37 doi 10.1158/0008-5472.CAN-09-3546.

39. Yamazaki CM, Yamaguchi A, Anami Y, Xiong W, Otani Y, Lee J*, et al.* Antibody-drug conjugates with dual payloads for combating breast tumor heterogeneity and drug resistance. *Nature Communications* 2021;**12**(1):3528 doi 10.1038/s41467-021-23793-7.

40. Barok Mr, Isola J, Pályi-Krekk Z, Nagy Pt, Juhász In, Vereb Gr*, et al.* Trastuzumab causes antibody-dependent cellular cytotoxicity–mediated growth inhibition of submacroscopic JIMT-1 breast cancer xenografts despite intrinsic drug resistance. *Molecular Cancer Therapeutics* 2007;**6**(7):2065-72 doi 10.1158/1535-7163.Mct-06-0766.

41. Clynes RA, Towers TL, Presta LG, Ravetch JV. Inhibitory Fc receptors modulate in vivo cytoxicity against tumor targets. *Nature Medicine* 2000;**6**(4):443-6 doi 10.1038/74704.

42. Spiridon CI, Guinn S, Vitetta ES. A comparison of the in vitro and in vivo activities of IgG and F(ab')2 fragments of a mixture of three monoclonal anti-Her-2 antibodies. *Clin Cancer Res* 2004;**10**(10):3542-51 doi 10.1158/1078-0432.Ccr-03-0549.

43. Breij EC, de Goeij BE, Verploegen S, Schuurhuis DH, Amirkhosravi A, Francis J*, et al.* An antibody-drug conjugate that targets tissue factor exhibits potent therapeutic activity against a broad range of solid tumors. *Cancer Res* 2014;**74**(4):1214-26 doi 10.1158/0008-5472.CAN-13-2440.

44. Challita-Eid PM, Satpayev D, Yang P, An Z, Morrison K, Shostak Y*, et al.* Enfortumab Vedotin Antibody-Drug Conjugate Targeting Nectin-4 Is a Highly Potent Therapeutic Agent in Multiple Preclinical Cancer Models. *Cancer Res* 2016;**76**(10):3003-13 doi 10.1158/0008-5472.CAN-15-1313.

45. Goldenberg DM, Cardillo TM, Govindan SV, Rossi EA, Sharkey RM. Trop-2 is a novel target for solid cancer therapy with sacituzumab govitecan (IMMU-132), an antibody-drug conjugate (ADC). *Oncotarget* 2015;**6**(26):22496-512 doi 10.18632/oncotarget.4318.

46. Ogitani Y, Hagihara K, Oitate M, Naito H, Agatsuma T. Bystander killing effect of DS-8201a, a novel anti-human epidermal growth factor receptor 2 antibody-drug conjugate, in tumors with human epidermal growth factor receptor 2 heterogeneity. *Cancer Sci* 2016;**107**(7):1039-46 doi 10.1111/cas.12966.

47. Scribner JA, Brown JG, Son T, Chiechi M, Li P, Sharma S*, et al.* Preclinical Development of MGC018, a Duocarmycin-based Antibody-drug Conjugate Targeting B7-H3 for Solid Cancer. *Mol Cancer Ther* 2020;**19**(11):2235-44 doi 10.1158/1535-7163.MCT-20-0116.

48. Yamato M, Hasegawa J, Maejima T, Hattori C, Kumagai K, Watanabe A*, et al.* DS-7300a, a DNA Topoisomerase I Inhibitor, DXd-Based Antibody-Drug Conjugate Targeting B7-H3, Exerts Potent Antitumor Activities in Preclinical Models. *Mol Cancer Ther* 2022;**21**(4):635-46 doi 10.1158/1535-7163.MCT-21-0554.

49. Zammarchi F, Corbett S, Adams L, Tyrer PC, Kiakos K, Janghra N*, et al.* ADCT-402, a PBD dimer-containing antibody drug conjugate targeting CD19-expressing malignancies. *Blood* 2018;**131**(10):1094-105 doi 10.1182/blood-2017-10-813493.

50. Deonarain MP, Yahioglu G, Stamati I, Pomowski A, Clarke J, Edwards BM*, et al.* Small-Format Drug Conjugates: A Viable Alternative to ADCs for Solid Tumours? *Antibodies (Basel)* 2018;**7**(2) doi 10.3390/antib7020016.

Figure 1. Endo180 is expressed on multiple sarcoma subtypes. a. Schematic of the Endo180 protein structure and mAb binding sites. CR, cysteine-rich domain, FNII, fibronectin type II domain, CTLD, C-type lectin-like domains. **b,c.** Soft tissue sarcoma (STS) tumor microarrays stained with the anti-Endo180 mAb 39.10. Panel b, representative images of Endo180-positive tumor cores from a total of 625 sarcoma patient samples, additional examples shown in Supplementary Fig. S1. Scale bars, 100 µm (whole core), 50 µm (enlarged inset). Panel c, bar chart showing proportion of tumors scored as Endo180-positive. **d.** *MRC2* expression from Barretina et al. (30) in normal fat (*n*=9), liposarcoma (de-differentiated) (*n*=46), leiomyosarcoma (*n*=26), undifferentiated pleomorphic sarcoma (UPS) (myxofibrosarcoma) (*n*=31), liposarcoma (myxoid) (*n*=20), liposarcoma (pleomorphic) (*n*=23) and UPS (pleomorphic) (*n*=3) (violin plots, red lines indicate median expression levels, dotted lines indicate upper and lower quartiles, Kruskal-Wallis test, Dunn's multiple comparison test). **e.** *MRC2* expression from Innovative Therapies for Children with Cancer (ITCC) samples in normal skeletal muscle *(n*=30) and rhabdomyosarcoma grouped as fusion negative (*n*=56), paired box 3-forkhead (PAX3-FKHR) fusion (*n*=34) and PAX7-FKHR fusion (*n*=10) (violin plots, red lines indicate median expression levels, dotted lines indicate upper and lower quartiles, one-way ANOVA test, Tukey's multiple comparison test).

Figure 2. A5/158 recognizes Endo180 expressed on sarcoma cell lines. **a.** Endo180 (*MRC2*) gene expression from Cancer Cell Line Encyclopedia (CCLE) in colorectal (*n*=70), breast cancer (*n*=61), soft tissue sarcoma (*n*=60) and bone sarcoma (*n*=39) cell lines (violin plots, red lines indicate median expression levels, dotted lines indicate upper and lower quartiles, Kruskal-Wallis test, Dunn's multiple comparison test). **b.** Western blot analysis of Endo180 in epithelial tumor (HT-29 and MCF-7) and sarcoma (MG-63, HT-1080, A-204, SJSA-1, SK-UT-1 and G-402) cell lines. Membranes were probed with anti-Endo180 mAb A5/158 (upper panel) or isotype control antibody (lower panel). Molecular size markers are in kDa. **c.** Confocal images

of sarcoma cell lines (MG-63 and HT-1080) and breast cancer cells (MCF-7) stained A5/158 or isotype control antibody directly conjugated to Alexa Fluor 488 (green). Nuclei were counterstained with DAPI (blue). Representative images out of two fields of view from experiments repeated on at least 3 occasions with equivalent findings. Scale bar, 50 μm.

Figure 3. A5/158 is suitable for intracellular drug delivery a. Confocal images of sarcoma and epithelial cells cultured with A5/158-488 (green) for 1 h at 4°C followed by incubation with LysoTracker Red (red) and Hoechst 33342 (blue) for 30 min at 37°C. White arrowheads indicate areas of green-red colocalization. Representative images out of two fields of view, from experiments repeated on at least 3 occasions with equivalent findings. Scale bar, 50 μm. **b.** Representative graphs of MG-63, HT-1080 and HT-29 cell growth (independent experiments; MG-63, *n*=3; HT-1080, *n*=2; HT-29, *n*=1) treated with A5/158 alone, A5/158-sb-saporin, Isotype-sb-saporin or saporin alone. MG-63 and HT-29 were cultured with 0.5 μg/mL of each treatment or molar equivalent of saporin alone for 144 h. HT-1080 was cultured with 1.5 μg/mL of each treatment or molar equivalent of saporin alone for 72 h (*n*=3 wells per condition, mean values ±SEM). Cell growth measured by confluency on the IncuCyte. **c.** At endpoint cell viability readouts were determined by CellTiter-Glo. Data is normalized to untreated cells (*n*=3 wells per condition, mean values ±SEM).

Figure 4. Endo180 expressing cell lines are sensitive to A5/158-vc-MMAE. a. Schematic representation of an antibody conjugated to an MMAE payload (green) via a cleavable valine-citrulline linker (pink). **b.** Endo180-positive and Endo180-negative cell lines were treated with A5/158-vc-MMAE or Isotype-vc-MMAE for 72 h. Shown are representative graphs (independent experiments *n*=3) of cell viability readouts determined by CellTiter-Glo. Data is normalized to untreated cells (*n*=3 wells per condition, mean values ±SEM).

Figure 5. A5/158-vc-MMAE impairs sarcoma tumor growth. a. Experimental schematic. 1 x 10^6 MG-63-mChLuc2 cells were injected subcutaneously (SC) into the flank of NSG mice. On day 14, once tumors reached ~3 mm in diameter, mice were randomized and began treatment. Mice were treated intravenously (IV) with 10 mg/kg of A5/158, Isotype-vc-MMAE, A5/158-vc-MMAE or vehicle (PBS) twice a week for a total of 4 doses (vehicle, *n*=3; A5/158, *n*=3; Isotype-vc-MMAE, *n*=5; A5/158-vc-MMAE *n*=5) (red arrows indicate treatment days). **b.** Bodyweight of treated mice relative to weight on day 0. **c.** Tumor growth in individual mice measured in tumor diameter and volume. **d.** Growth rate of tumors (one-way ANOVA, Tukey's multiple comparison test). Data shown are mean values ±SEM **e.** Final tumor volumes (Kruskal-Wallis, Dunn's multiple comparison test) and weights (one-way ANOVA, Tukey's multiple comparison test). All shown as mean values ±SEM**. f.** E*x vivo* images of MG-63 tumors. Scale bar, 10 mm. **g**. Representative immunohistochemistry images of MG-63 tumors stained for Endo180. Scale bar, 50 µm. **h**. Relative Endo180 (*MRC2*) expression of MG-63 tumors after treatment in comparison to parental MG-63 cells *in vitro,* analyzed by RT-qPCR and normalized to *UBC* endogenous control. Data shown are mean values ±SEM.

Figure 6. A5/158-vc-MMAE decreases the number and size of spontaneous metastases. Continuation of Fig. 5. **a.** *Ex vivo* IVIS imaging and quantification of lungs at end point (mean values ±SEM, two-sided Mann-Whitney *U* test). **b.** Representative FFPE lung sections stained for lamin A/C at 3 levels 150 µm apart. Scale bar, 100 µm. **c.** Quantification of the number of metastatic lung lesions, average area of lung lesions and % metastatic area of lung lesions (mean of three sections per mouse). Data shown are mean values ±SEM; number of lung lesions, two-sided Mann-Whitney U test; average area of lung lesions and metastatic tumor area, two-sided unpaired *t*-test. **d**. Proportion of mice with liver metastases. **e.** Proportion of mice with lymph node metastases.

Figure 1

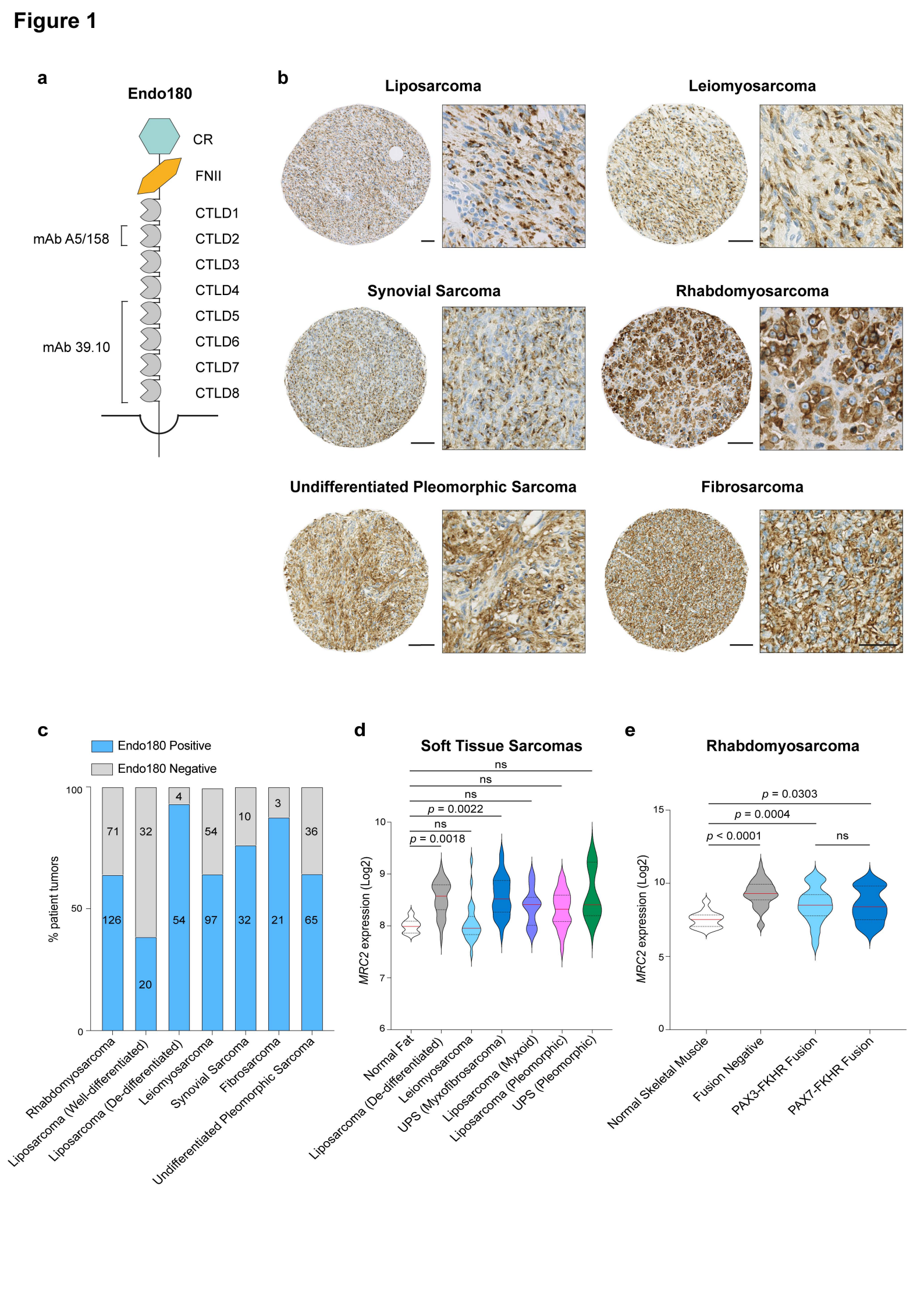
a
Endo180
CR
FNII
CTLD1
CTLD2
CTLD3
CTLD4
CTLD5
CTLD6
CTLD7
CTLD8
mAb A5/158
mAb 39.10
b
Liposarcoma
Leiomyosarcoma
Synovial Sarcoma
Rhabdomyosarcoma
Undifferentiated Pleomorphic Sarcoma
Fibrosarcoma
c
Endo180 Positive
Endo180 Negative
% patient tumors
100
50
0
71
126
32
20
4
54
54
97
10
32
3
21
36
65
Rhabdomyosarcoma
Liposarcoma (Well-differentiated)
Liposarcoma (De-differentiated)
Leiomyosarcoma
Synovial Sarcoma
Fibrosarcoma
Undifferentiated Pleomorphic Sarcoma
d
Soft Tissue Sarcomas
MRC2 expression (Log2)
ns
ns
ns
p = 0.0022
ns
p = 0.0018
Normal Fat
Liposarcoma (De-differentiated)
Leiomyosarcoma
UPS (Myxofibrosarcoma)
Liposarcoma (Myxoid)
Liposarcoma (Pleomorphic)
UPS (Pleomorphic)
e
Rhabdomyosarcoma
MRC2 expression (Log2)
p = 0.0303
p = 0.0004
p < 0.0001
ns
Normal Skeletal Muscle
Fusion Negative
PAX3-FKHR Fusion
PAX7-FKHR Fusion

Figure 2

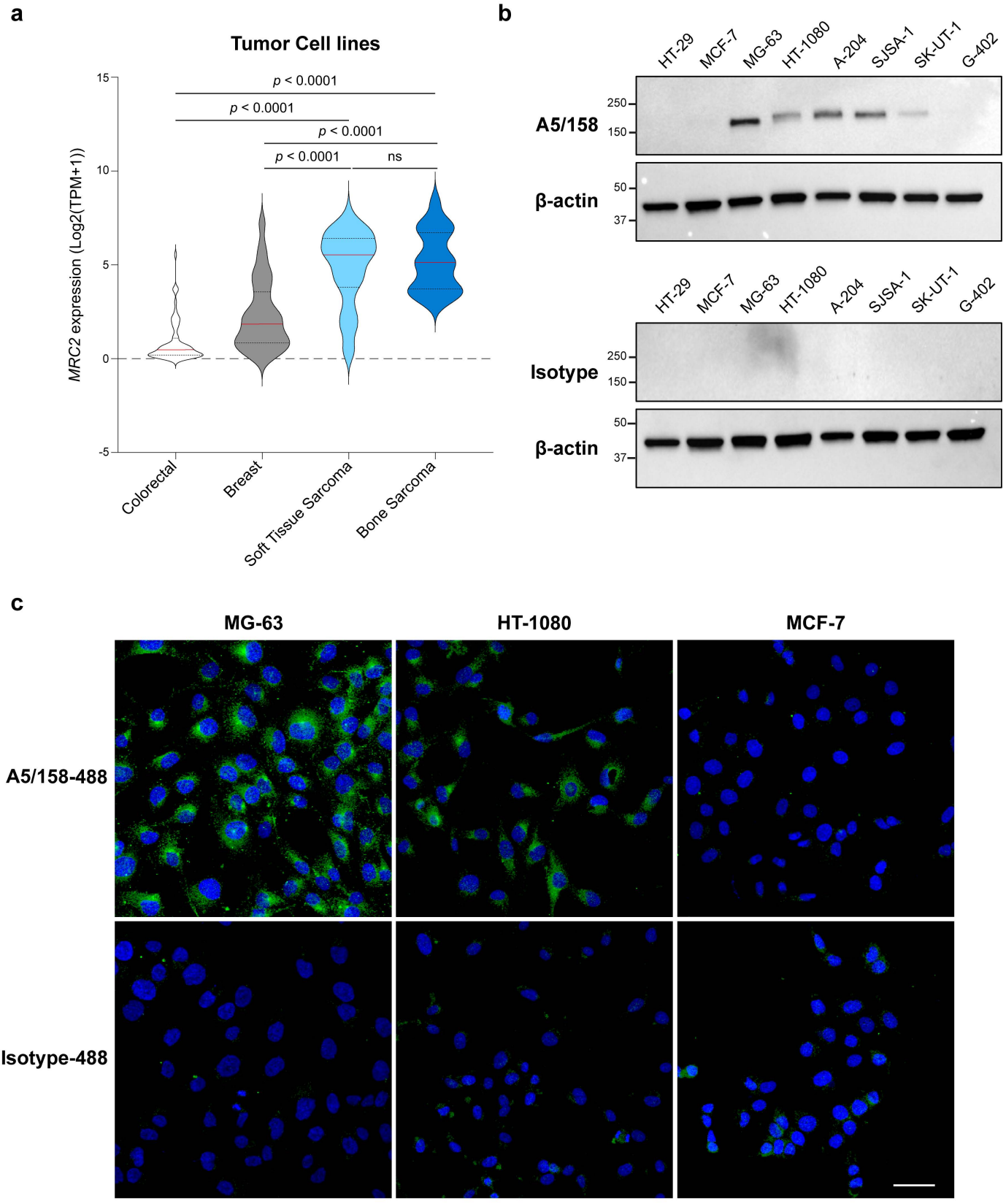
a
Tumor Cell lines
p < 0.0001
p < 0.0001
p < 0.0001
p < 0.0001
ns
MRC2 expression (Log2(TPM+1))
15
10
5
0
-5
Colorectal
Breast
Soft Tissue Sarcoma
Bone Sarcoma
b
HT-29
MCF-7
MG-63
HT-1080
A-204
SJSA-1
SK-UT-1
G-402
A5/158
250
150
β-actin
50
37
Isotype
c
MG-63
HT-1080
MCF-7
A5/158-488
Isotype-488

Figure 3

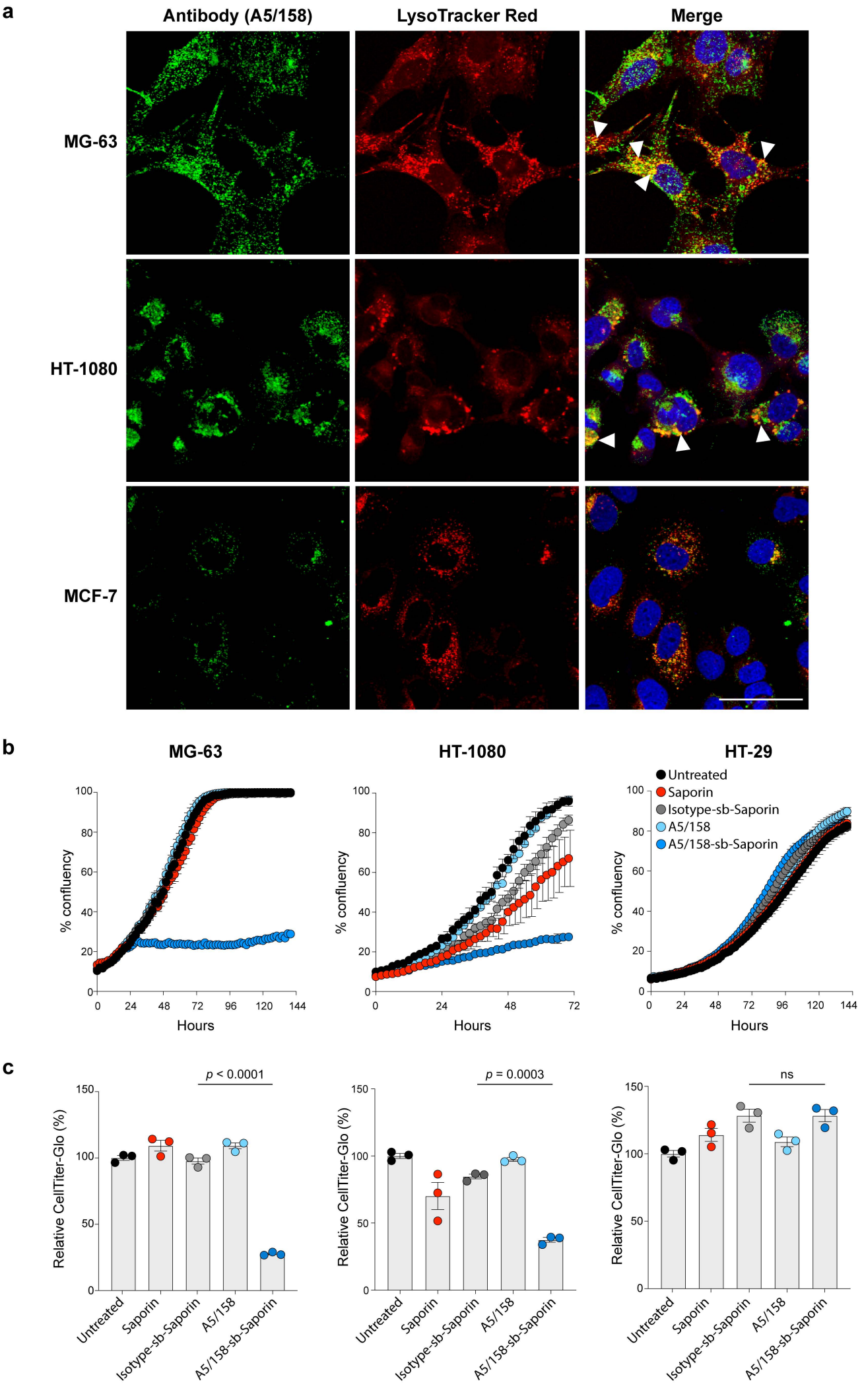
a
Antibody (A5/158)
LysoTracker Red
Merge
MG-63
HT-1080
MCF-7
b
MG-63
HT-1080
HT-29
% confluency
Hours
Untreated
Saporin
Isotype-sb-Saporin
A5/158
A5/158-sb-Saporin
c
Relative CellTiter-Glo (%)
p < 0.0001
p = 0.0003
ns
Untreated
Saporin
Isotype-sb-Saporin
A5/158
A5/158-sb-Saporin

Figure 4

a

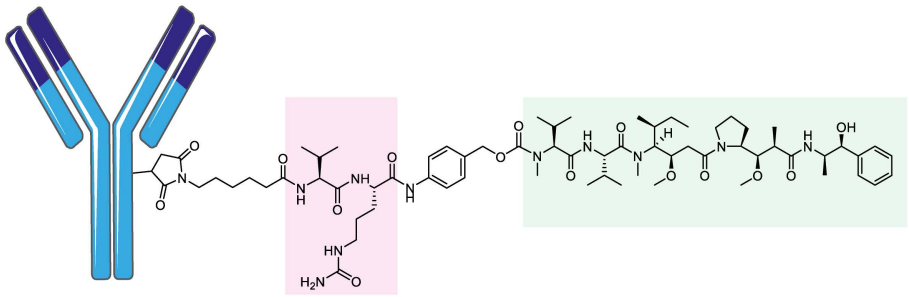

Antibody
A5/158, Isotype

Linker
Valine-Citrulline

Drug
MMAE

b

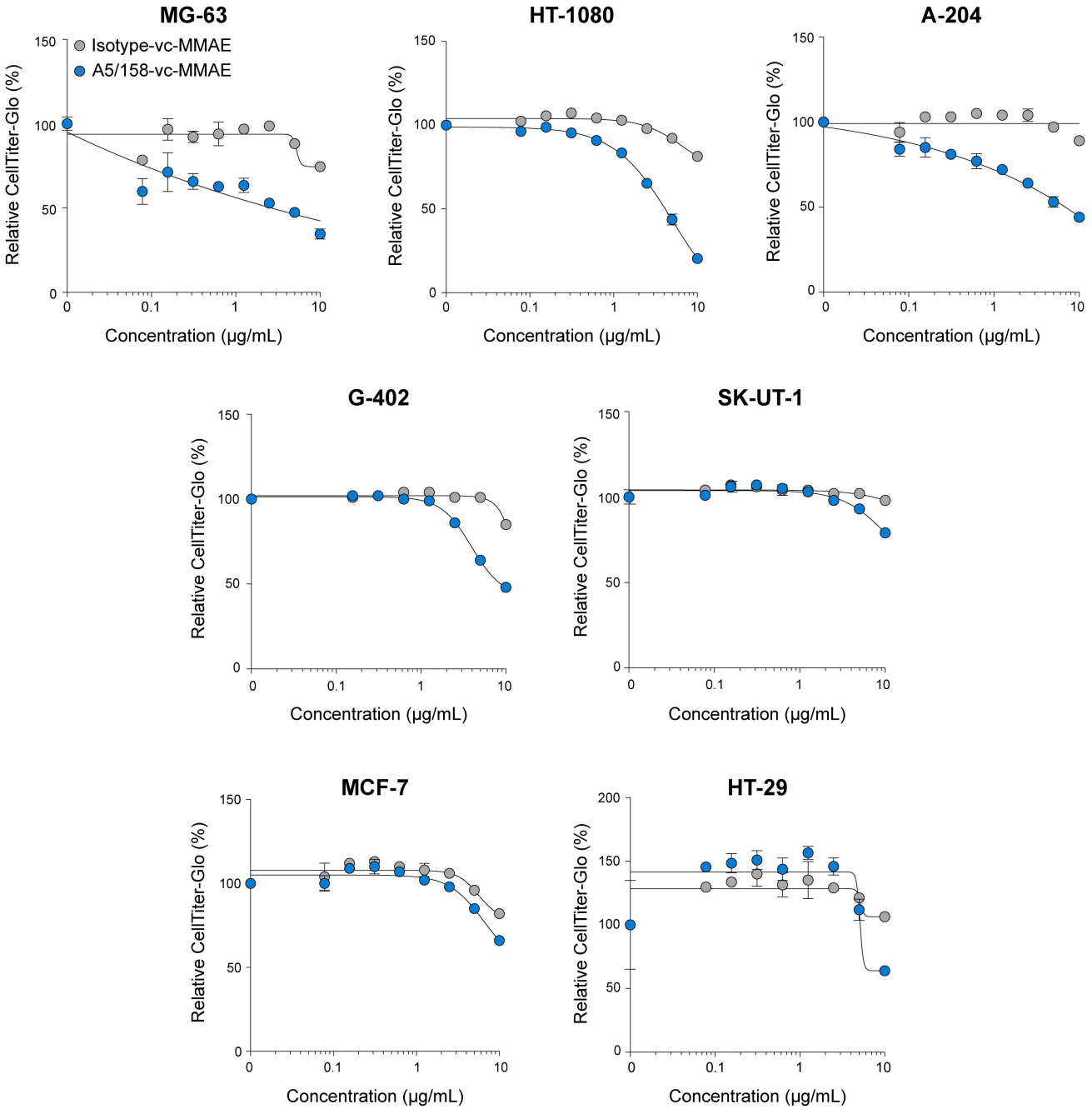

Figure 5

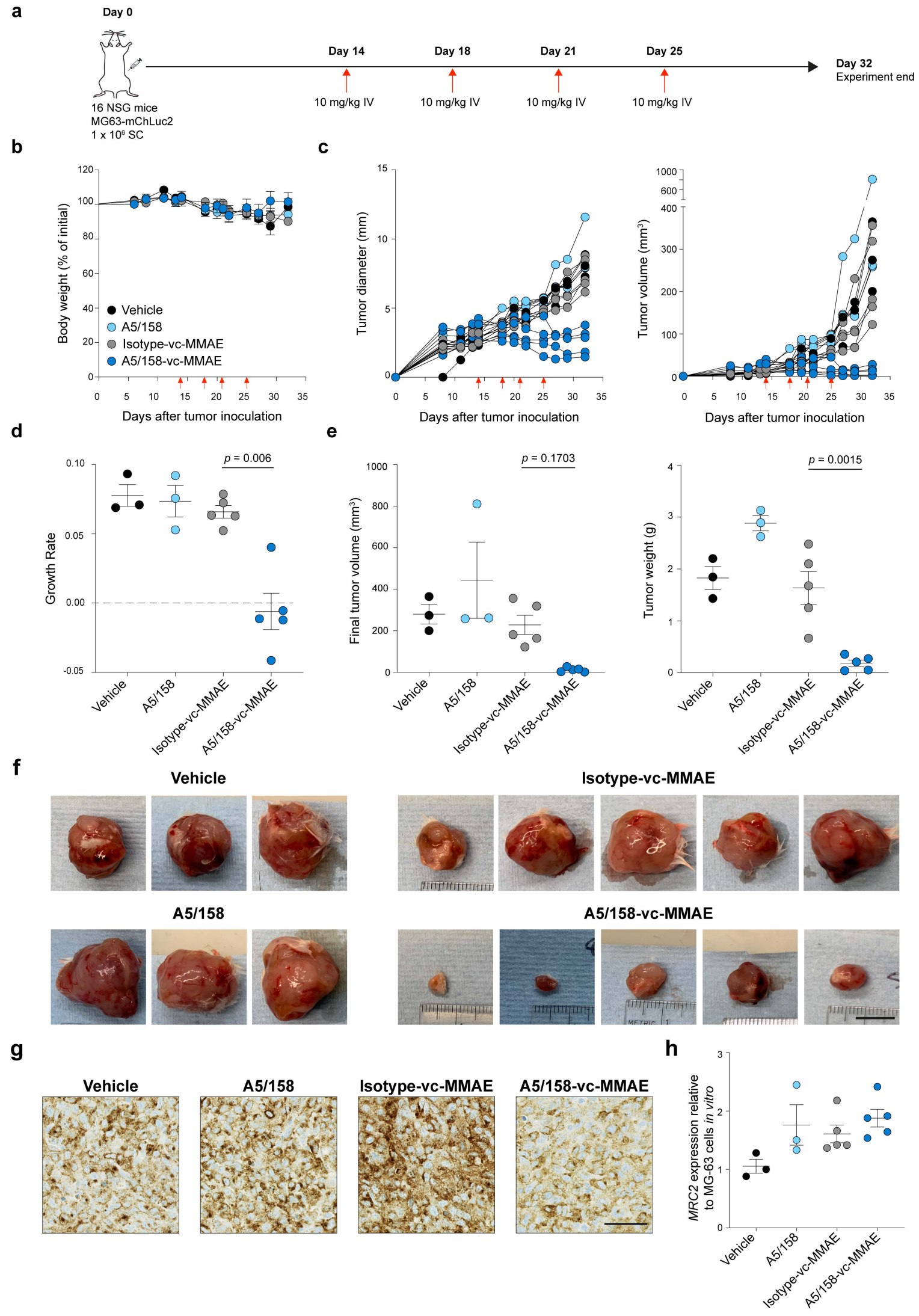
a
Day 0
16 NSG mice
MG63-mChLuc2
1 x 10⁶ SC
Day 14
Day 18
Day 21
Day 25
10 mg/kg IV
10 mg/kg IV
10 mg/kg IV
10 mg/kg IV
Day 32
Experiment end
b
Body weight (% of initial)
Vehicle
A5/158
Isotype-vc-MMAE
A5/158-vc-MMAE
Days after tumor inoculation
c
Tumor diameter (mm)
Days after tumor inoculation
Tumor volume (mm³)
Days after tumor inoculation
d
p = 0.006
Growth Rate
Vehicle
A5/158
Isotype-vc-MMAE
A5/158-vc-MMAE
e
p = 0.1703
Final tumor volume (mm³)
p = 0.0015
Tumor weight (g)
f
Vehicle
Isotype-vc-MMAE
A5/158
A5/158-vc-MMAE
g
Vehicle
A5/158
Isotype-vc-MMAE
A5/158-vc-MMAE
h
MRC2 expression relative to MG-63 cells in vitro

Figure 6

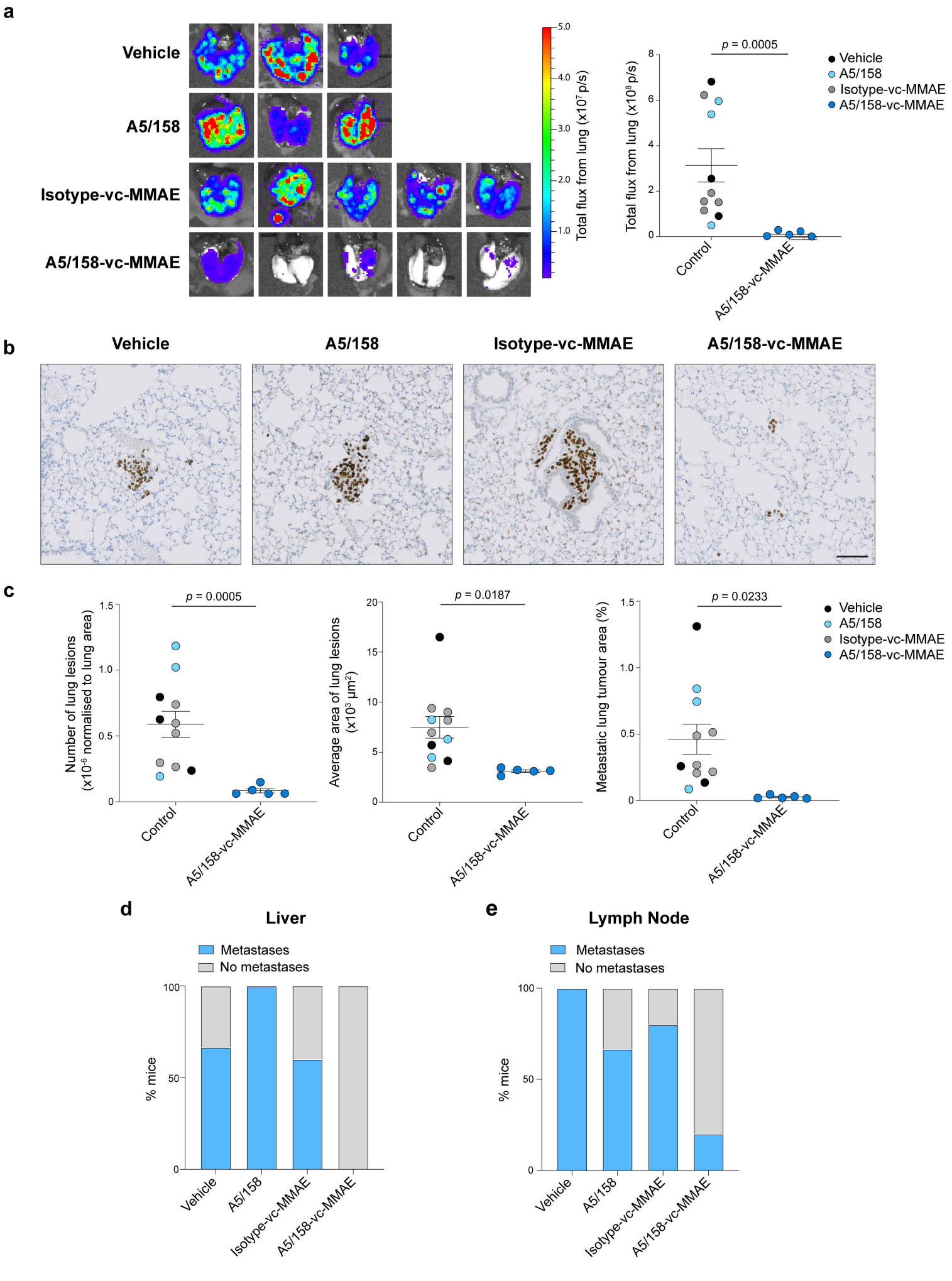
a
Vehicle
A5/158
Isotype-vc-MMAE
A5/158-vc-MMAE
Total flux from lung (x10⁷ p/s)
5.0
4.0
3.0
2.0
1.0
p = 0.0005
Total flux from lung (x10⁸ p/s)
Control
A5/158-vc-MMAE
Vehicle
A5/158
Isotype-vc-MMAE
A5/158-vc-MMAE
b
Vehicle
A5/158
Isotype-vc-MMAE
A5/158-vc-MMAE
c
p = 0.0005
Number of lung lesions (x10⁻⁶ normalised to lung area)
p = 0.0187
Average area of lung lesions (x10³ µm²)
p = 0.0233
Metastatic lung tumour area (%)
Control
A5/158-vc-MMAE
Vehicle
A5/158
Isotype-vc-MMAE
A5/158-vc-MMAE
d
Liver
Metastases
No metastases
% mice
Vehicle
A5/158
Isotype-vc-MMAE
A5/158-vc-MMAE
e
Lymph Node
Metastases
No metastases
% mice
Vehicle
A5/158
Isotype-vc-MMAE
A5/158-vc-MMAE